ADVANCES IN INORGANIC CHEMISTRY, VOL. 32

NICKEL IN METALLOPROTEINS

R. CAMMACK

Department of Biochemistry, King's College London (KQC), University of London, Kensington, London W8 7AH, England

I. Introduction

Nickel has long been suspected to be an essential trace element for living organisms, but the identification of its functions in molecular terms is relatively recent. The first nickel protein to be identified was urease (urea ammonia hydrolase) (*1*). This was demonstrated 49 years after the original isolation and crystallization of the enzyme by Sumner (*2*). This enzyme is of widespread occurrence, and the specific requirement for nickel explains many of the effects of nickel deficiency in plants (*3, 4*).

Certain bacteria—in particular hydrogen bacteria, methanogens, and acetogens—were found to have a relatively high demand for nickel as a trace element. This was not recognized at first, since the requirement could be satisfied by nickel dissolved from stainless-steel culture apparatus (*5*). These chemolithotrophic bacteria are named from the metabolic processes by which they obtain energy for growth. All of them use hydrogen as reductant, in different ways. The hydrogen bacteria, such as *Alcaligenes* and *Nocardia*, are aerobes and catalyze the oxidation of hydrogen. Methanogens, of which the best-studied genera are *Methanobacterium* and *Methanosarcina*, are anaerobes which convert carbon dioxide to methane, using reducing agents such as hydrogen gas (*6*). The acetogens, such as *Clostridium thermoaceticum*, *Clostridium aceticum*, and *Acetobacterium woodii* (25), are also strict anaerobes and catalyze the conversion of carbon dioxide and carbon monoxide to acetic acid using hydrogen and other reductants.

The requirement for nickel was explained when it was found that the enzyme hydrogenase contains nickel. A characteristic EPR spectrum observed in membranes of methanogenic bacteria was recognized by Lancaster as being due to nickel (*7, 8*). This assignment was confirmed by growing the cells on the stable isotope ^{61}Ni, which has a nuclear spin $I = 3/2$, and observing the hyperfine splitting of the spectrum into four lines (*9*). Similar spectra have been observed in hydrogenases from sulfate-reducing bacteria (*10, 11*), photosynthetic bacteria (*12*), and hydrogen-oxidizing bacteria (*13*).

Hydrogenases are enzymes that catalyze the production or consumption of hydrogen gas. Not all hydrogenases contain nickel, and in some of those that contain nickel, the nickel is EPR silent (*14*). Properties of a few of the known Ni hydrogenases are summarized in Table I; more comprehensive listings are given in Refs. *15* and *16*. The composition and biological function of hydrogenases have been reviewed recently (*15–18*), and this review will concentrate on the chemistry of those nickel centers.

In the methanogenic bacteria, nickel is also involved in a second process, in which a complex series of reactions leads to the release of methane gas (*19–21*). The enzyme involved, methyl-coenzyme M reductase, contains a cofactor F_{430} which is a nickel–porphinoid complex. The methanogens belong to an unusual group of bacteria described as Archaebacteria, which appear to be very ancient (*22*). Like the acetogens they are strict anaerobes. Although they are now restricted in habitat, these organisms, with their metabolism involving nickel and the related cobalamins, may have played an important part in the early phases of evolution.

TABLE I

COMPOSITION AND SPECTROSCOPIC PROPERTIES OF TYPICAL Ni HYDROGENASES

Organism	Type of hydrogenase	Center	Paramagnetic state
Methanobacterium thermoautotrophicum (methanogenic bacterium)	Soluble, deazaflavin reducing	Ni	Oxidized, Ni(III); H_2 reduced, Ni(I)?
		2–3[4Fe–4S]	EPR silent?
Desulfovibrio gigas (sulfate-reducing bacterium)	Soluble, periplasmic	Ni	Oxidized, Ni(III), Ni-A; H_2 reduced, Ni(I)?, Ni-C
		[3Fe–xS]	Oxidized
		[4Fe–4S]	Reduced
Chromatium vinosum (anaerobic photosynthetic bacterium)	Membrane bound	Ni	Oxidized, Ni(III), Ni-a; H_2 reduced, Ni(I)
		[3Fe–xS] or [4Fe–4S]	Oxidized
Nocardia opaca (hydrogen-oxidizing bacterium)	Soluble, NAD reducing	Ni	EPR silent
		[3Fe–xS]	Oxidized
		3[4Fe–4S]	Reduced
		[2Fe–2S]	Reduced
		FMN	Semiquinone radical

A third nickel-containing enzyme found in some strictly anaerobic bacteria is involved in the oxidation of carbon monoxide to carbon dioxide, and in the formation of acetyl-coenzyme A from carbon monoxide (*23, 24*). This reaction was reported to occur in sewage sludge in 1932 by Fischer (*102*), who was one of the cooriginators of the Fischer–Tropsch synthesis of hydrocarbons from carbon monoxide. It has been given the trivial name carbon monoxide dehydrogenase, but this seems illogical in view of the fact that carbon monoxide contains no hydrogen. In this review the alternative name carbon monoxide oxidoreductase will be used. Since the principal function of the enzyme is probably to synthesize acetyl-coenzyme A, the name "acetyl-CoA synthase" is also appropriate. It is a major enzyme of acetogenic bacteria, which have a novel pathway for fixation of CO_2 (*26, 27*), and it is also found in methanogens.

Both hydrogenases and carbon monoxide oxidoreductases contain iron–sulfur clusters in addition to nickel. It may be noted that in addition to the Ni hydrogenases, there is another class of Fe hydrogenases, such as those in clostridia, which contain no nickel but have a specialized type of iron–sulfur cluster (*28a, 28b*). Therefore, it has to be established that the nickel in Ni hydrogenases is the active site; as will be seen later, there is a considerable amount of circumstantial evidence for this.

A recent review by Hausinger (*29*) deals with nickel utilization by microorganisms. In addition to known effects of nickel deficiencies, nickel and its compounds are known to have toxic and carcinogenic effects. The reader is referred to recent proceedings (*30a, 30b*).

II. Urease

A. Composition

The first enzyme that was demonstrated to contain nickel was urease (urea amidohydrolase) from jack bean. It catalyzes the hydrolysis of urea to ammonia and carbon dioxide. The protein has a multimeric structure with a relative molecular mass of 590,000 Da. Analysis indicated 12 nickel atoms/mol. Binding studies with the inhibitors indicated an equivalent weight per active site of 105,000, corresponding to 2 nickel atoms/active site. During removal of the metal by treatment with EDTA at pH 3.7, the optical absorption and enzymatic activity correlated with nickel content. This, combined with the sensitivity of the enzyme to the chelating agents acetohydroxamic acid and phosphoramidate, indicates that nickel is essential to the activity of the enzyme (*1*).

B. Spectroscopic Properties

The nickel in urease is nonmagnetic and appears to be in the oxidation state Ni(II). The broad optical absorption spectrum is influenced by ligands to the metal (Fig. 1). The spectrum obtained in the presence of the competitive inhibitor mercaptoethanol, after correction for Rayleigh scattering by the protein (*31*), shows absorption peaks at 324, 380, and 420 nm, with molar absorption coefficients of 1550, 890, and 460 M^{-1} cm^{-1}, respectively. These were assigned to sulfur-to-nickel charge transfer transitions. The spectrum is changed by addition of other inhibitors, such as acetohydroxamic acid (Fig. 1B). Similar

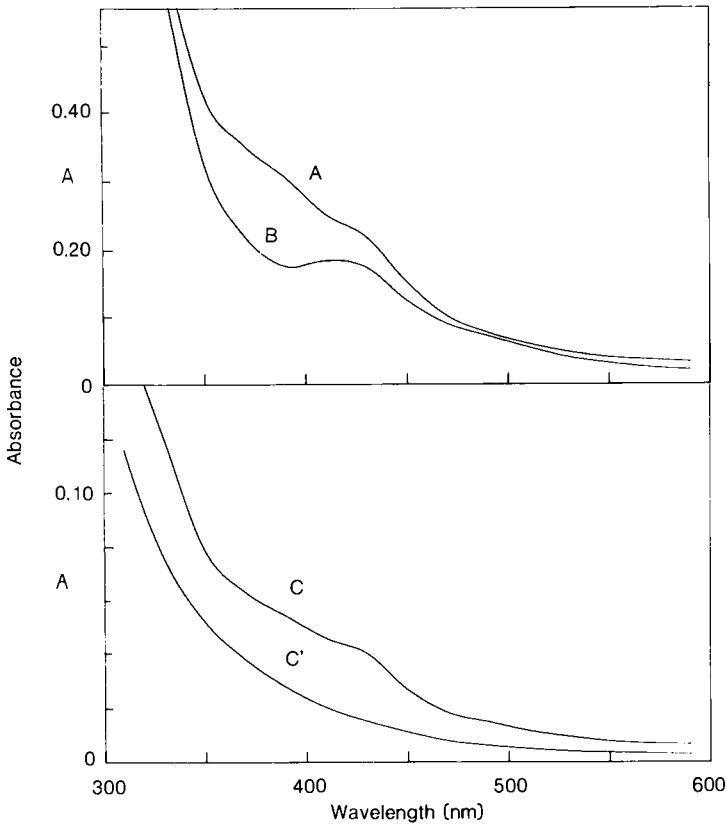

FIG. 1. Optical absorption spectra of urease from jack bean (*Canavalia ensiformis*). (A) Enzyme, 43.3 mg/ml in 1 m*M* β-mercaptoethanol/1 m*M* EDTA; (B) with 10 m*M* acetohydroxamic acid; (C) urease, 11.9 mg/ml after acidification, pH 3.8; (C') after 2 hours at pH 3.8; the latter enzyme retained 6.1% of its original activity. Redrawn, with permission, from Ref. *1*.

spectra have been observed in other nickel-protein complexes, including Ni(II) carboxypeptidase, which also undergoes spectra changes on addition of the inhibitor β-phenyl propionate (*32*). The spectra of urease have been interpreted in terms of an octahedral site (*31a*), although the site in carboxypeptidase, occupied by nickel, is coordinated to one cysteine sulfur, two histidine imidazoles, and the carboxylate of a glutamate residue (*32a*).

In extended X-ray absorption fine structure (EXAFS) studies of urease, Hasnain, Piggott, and co-workers (*33, 34*) demonstrated that spectra were similar to those of benzimidazole complexes, consistent

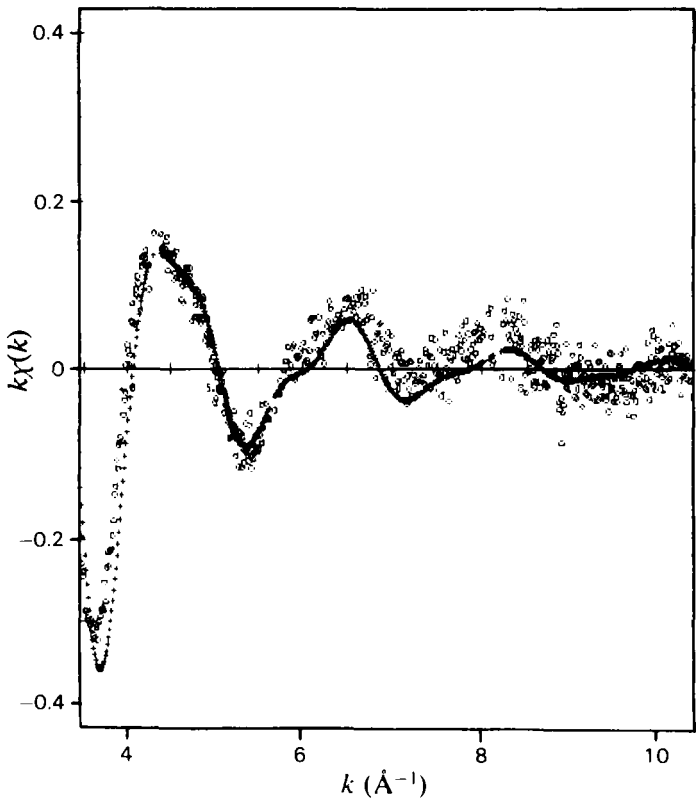

FIG. 2. Ni K-edge EXAFS spectrum of urease. The curve (+) is calculated for a single type of nickel site, and the minimization of parameters was based on those for the model complexes Ni(1-*n*-propyl-2-hydroxybenzylbenzimidazole)$_3$(ClO_4) and Ni(2-hydroxymethylbenzimidazole)$_3Br_2$. Atoms (with distances in nanometers given in parentheses) in the simulation were N (0.204), O (0.206), O (0.225), C (0.294), C (0.312), N (0.392), and C (0.394). Reproduced, with permission, from Ref. *34*.

with nickel coordination to histidine nitrogen and oxygen ligands. The spectra obtained for urease (Fig. 2) are presumably the average of two types of sites.

C. Mechanism of Catalysis

Dixon *et al.* (*35*) have proposed a mechanism for urease catalysis (Fig. 3) based on studies of the reactions with the poor substrates formamide, acetamide, and *N*-methylurea. They suggest that the two nickel ions are both in the active site, one binding urea and the other a hydroxide ion which acts as an efficient nucleophile. This implies that the nickel ions are within 0.6 nm (1 nm = 10 Å) of each other; so far it

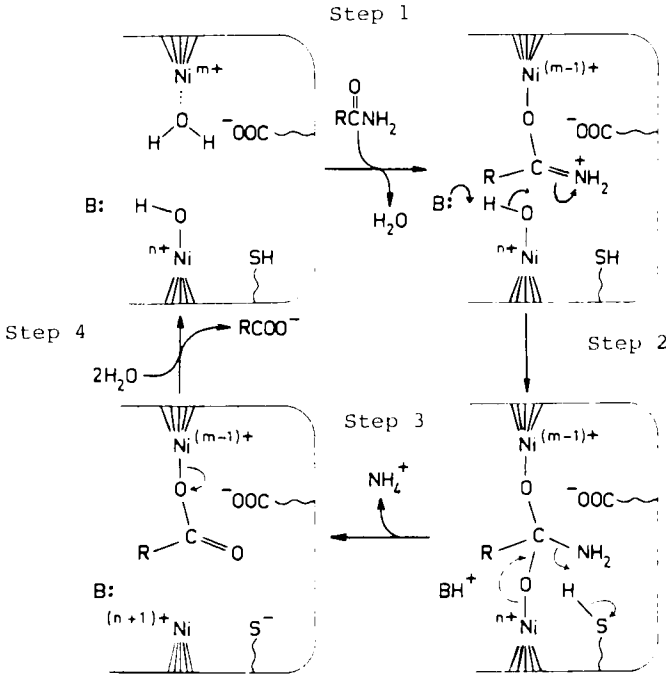

FIG. 3. Proposed reaction cycle for urease. For urea, R = $-NH_2$. Step 1: urea is activated toward nucleophilic attack by O coordination to a nickel ion; the $=N^+H_2$ is stabilized by interaction with a protein carboxylate. Step 2: nucleophilic attack by a hydroxide ion, coordinated to the second nickel, to form a tetrahedral intermediate. Step 3: breakdown of the tetrahedral intermediate to form a coordinated carbamate ion. Step 4: hydrolysis releases carbamate ion, the initial product of urease on urea. Reproduced, with permission, from Ref. *34*.

has not been possible to confirm this spectroscopically. The reaction is analogous with peptide hydrolysis by carboxypeptidase, in which a hydroxide ion bound to a zinc ion has been implicated.

III. Hydrogenase

A. Types of Hydrogenases

In contrast to urease the nickel in other bacterial enzymes appears to have a redox function and to take up oxidation states Ni(I) and/or Ni(III). Fortunately these states have recently become better understood in inorganic systems (see the preceding review in this volume by A. G. Lappin and A. McAuley).

The Ni hydrogenases are now the most intensively studied nickel proteins. Although they have only been investigated for a few years, there is a considerable amount of evidence about the state and function of nickel in the catalytic cycle (*16*). In fact, "hydrogenase" is not one enzyme, but a class of enzymes. Hydrogenases may be distinguished functionally, in that they serve to produce or consume hydrogen in reactions with various physiological electron acceptors and donors. They may also be distinguished by the following molecular and catalytic properties.

1. Types of iron–sulfur clusters and other groups, such as flavin or selenium, that are present.
2. Types of EPR signals due to nickel.
3. Sensitivity to deactivation by oxygen and, in some cases, slow, reductive reactivation.
4. Different ratio of products in hydrogen isotope-exchange assays.

Among the diversity of Ni hydrogenases, there is a common pattern of protein composition, to which most conform, which consists of two protein subunits of relative molecular mass approximately 60,000 and 30,000 Da (*14*). There is some evidence (*38*) that the nickel is situated in the 60,000-Da subunit. More complex hydrogenases, such as the soluble hydrogenase of *Nocardia opaca* (Table I), contain other subunits which are concerned with the reduction of specific electron acceptors.

B. EPR Spectroscopic Properties of Nickel

The coordination and oxidation state of nickel in hydrogenase are difficult to determine, because the optical spectra are obscured by the

iron–sulfur clusters and because the commonest oxidation state Ni(II) is EPR silent. However, as already noted, some hydrogenases show significant EPR signals, which are the best indicators at present of the function of nickel in these enzymes. In the following discussion, EPR spectra will be described with reference to the typical spectra from *Desulfovibrio gigas* hydrogenase, and any differences in other Ni hydrogenases will be noted.

Examples of EPR spectra of the Ni hydrogenase from *D. gigas* are shown in Fig. 4. This hydrogenase, in common with those from *Methanobacterium thermoautotrophicum* (*7, 9, 39*) and *Chromatium*

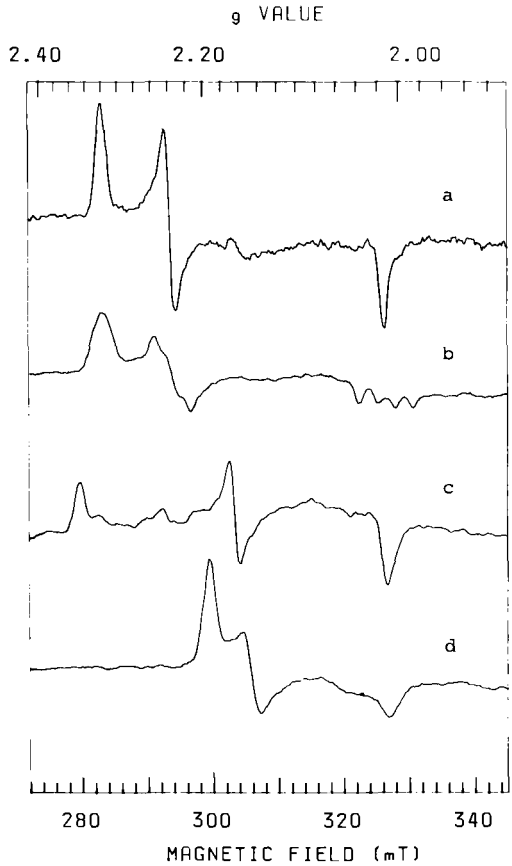

FIG. 4. EPR spectra of nickel in *D. gigas* hydrogenase: (a) Ni-A, enzyme stored under air; (b) Ni-A, enzyme enriched with ^{61}Ni; (c) Ni-B, enzyme-activated enzyme reoxidized with dichloroindophenol at pH 7.8; (d) Ni-C, enzyme activated under hydrogen. Spectra were recorded at a temperature of approximately 100 K, with microwave power 10 mW.

vinosum (*12*) shows a prominent EPR signal with g values of 2.32, 2.21, and 2.01 (Fig. 4a). In *D. gigas* this spectrum has been termed Ni-A (*40, 41*). Frequently a second minor signal is observed in oxidized hydrogenase, termed Ni-B in *D. gigas* (Fig. 4b). In *C. vinosum* hydrogenase, the corresponding signals have been termed Ni-a and Ni-b. It may be mentioned that a number of additional EPR signals have been reported, in particular hydrogenases from various bacteria, the origins of which are not clear at present, and which will not be described here.

It is generally believed that the EPR-detectable nickel in oxidized hydrogenase represents low-spin Ni(III), d^7. In support of this view, the EPR signal disappears on reduction, consistent with reduction to Ni(II). The g values of oxidized hydrogenase were interpreted by Lancaster (*7*) as due to a rhombically distorted octahedron with the unpaired electron in a $d_x{}^2$ orbital. Square–pyramidal geometry is also possible. In practice, the coordination sites in proteins are often so distorted that structural interpretations of EPR spectra based on crystal symmetry may be misleading.

When the hydrogenases of *D. gigas* (*42*), *M. thermoautotrophicum* (*39*), or *C. vinosum* (*43*) are progressively reduced by hydrogen, the EPR spectra indicate three stages: first, the Ni-A and Ni-B signals disappear; then a signal (termed Ni-C in *D. gigas*) appears (Fig. 4d); then finally this signal also disappears. The Ni-C signal represents an intermediate oxidation state since it can be restored by flushing away excess hydrogen with argon (*39, 41, 43*).

C. Midpoint Redox Potentials

The midpoint reduction potentials of the various EPR-detectable nickel species in hydrogenase are all less than 0 mV versus the standard hydrogen electrode (Table II). This is in contrast to synthetic inorganic complexes with amino acids (*44*), in which the oxidation of Ni(II) to Ni(III) occurs at much higher potentials (0.8–1.2 mV) and is accompanied by reorganization of the complex (*45*). This requires some explanation in view of the interpretation of the Ni-A EPR signal as Ni(III)(*7*).

There are various factors which might stabilize the Ni(III) state and thus lower the Ni(III)/Ni(II) potential, the first of these being sulfur ligation, for which there is spectroscopic evidence (Section II,D,1,2). The ligands to nickel in the above-mentioned amino acid complexes are oxygen and nitrogen. Moreover, it is well established that, for a transition metal center with a particular arrangement of ligands, a protein environment can adjust the midpoint potential over a range of

TABLE II

MIDPOINT REDOX POTENTIALS OF HYDROGENASES[a]

Hydrogenase	Redox process	E_m (mV)	E_m/pH unit (mV)
D. gigas (*65*)	Reduction of Ni-A	−150	−60
	Reduction of [3Fe−*x*S]	−35	0
	Reduction of [4Fe−4S][b]	−350	−60
	Appearance of Ni-C	−270	−120
	Disappearance of Ni-C	−390	−60
	Reductive activation (*75*)	−310	−60
	Oxidative deactivation (*99*)	−133	−60
C. vinosum	Reduction of Ni-a	−175 (*43*) (pH 7.3)	ND
	Reduction of [3Fe−*x*S][c]	−20 (*100*), −165 (*43*) (pH 7.3)	0
	Disappearance of interaction between Ni and [3Fe−*x*S]	180 (*100*), −29 (*43*) (pH 7.3)	−60
N. opaca (*82*)	Reduction of [4Fe−4S][d]	−420	ND
	Reduction of [2Fe−2S][d]	−285	ND
	Reduction of [3Fe−*x*S]	25	ND

[a] Potentials are values at pH 7.0, expressed relative to the standard hydrogen electrode. ND, Not determined. Numbers in parentheses are references.

[b] The redox potential of the [4Fe−4S] cluster in *D. gigas* hydrogenase is inferred from an extremely broad EPR signal in the reduced enzyme, which correlates with the splitting of the Ni-C signal (*65*).

[c] The $g = 2.01$ signal in *C. vinosum* hydrogenase is interpreted by Albracht *et al.* (*12*) as a [4Fe−4S] cluster which changes to a [3Fe−*x*S] cluster when interaction with the nickel center ceases.

[d] The EPR-detectable iron–sulfur clusters of *N. opaca* hydrogenase are associated with the NAD-reducing segment of the enzyme.

several hundred millivolts by means of electrostatic and other effects (*46*). There are other mechanisms known from chemical complexes which would also lower the potential (*47*). A confined binding site would have this effect, as has been demonstrated in Ni complexes with macrocycles (*48*). However, it may be difficult to achieve this in the more flexible environment of a protein.

The opposite problem occurs if we are to invoke Ni(I) as a participant in the reaction cycle, since the Ni(II)/Ni(I) couple is generally more negative, by about 1 V, than Ni(III)/Ni(II)(*37*). In some hydrogenases, such as in *D. gigas,* it is known that the enzyme undergoes a slow conformational change during conversion to the active state, in which the alleged Ni(I) EPR signal appears (e.g., see Ref. *49*), so the altered conformation might stabilize the Ni(I) state. The Ni(I) state is stabilized, relative to the Ni(II) state, by ligands which favor tetrahedral coordination. Dietrich-Buchecker *et al.* (*50*) have obtained stable Ni(I) complexes by using catenand ligands, containing interlocking, 30-membered, coordinating rings.

D. Coordination State of Nickel

In those hydrogenases in which the nickel is EPR detectable (Table I), the remarkable similarity in the lineshapes of the spectra is a strong indication that the nickel environment is highly conserved. Therefore, although there are substantial differences in the catalytic activities and specificity of hydrogenases from different organisms, it seems likely that there are, at most, only a few different types of nickel centers. It therefore seems reasonable to correlate spectroscopic information on nickel in hydrogenases from different species in order to obtain a composite picture.

It is not known at present if the nickel is coordinated directly to the protein, as in copper and iron–sulfur proteins, or to an organic cofactor, as in the molybdenum hydroxylases and hemoproteins.

1. X-Ray Absorption Spectroscopy

X-Ray absorption edge spectra and EXAFS measurements have the potential for detailed determination of the coordination geometry of the nickel sites. Nickel K-edge X-Ray absorption measurements have so far been made on two hydrogenases. At present there are few suitable model compounds containing Ni(III) or Ni(I) with sulfur ligands, and the interpretations as to coordination geometry and oxidation state should therefore be regarded as preliminary.

EXAFS studies of the F_{420}-reducing hydrogenase from *M. thermoautotrophicum* (*51*) indicated that sulfur was the principal scattering nucleus. Best fits to the data were obtained with 2.9 sulfur atoms, at a distance of approximately 0.225 nm. The spectra were refined with the aid of data from Ni(II)(toluene-3, 4-dithiolato)$_2^{2-}$, in which the Ni–S distance was estimated to be 0.219 nm. Lindahl *et al.* (*51*) note that because of differences between the Debye–Waller factors of the enzyme and model compound, there is uncertainty about the exact number of sulfur ligands involved. Scattering by nuclei of other ligands to nickel, such as oxygen or nitrogen, of lower atomic mass, was expected to be so weak that they could not be resolved.

In *D. gigas* hydrogenase, X-ray absorption edge measurements gave a −2-eV shift in the nickel K-edge on reduction of the sample by hydrogen (*52*). This was similar to the difference between the model compounds [Ni(III)(maleonitriledithiolate)$_2$](n-Bu_4N) and [Ni(II)-(maleonitriledithiolate)$_2$](n-$Bu_4N)_2$, and was taken as evidence for reduction of Ni(III) to Ni(II) in hydrogenase. It is difficult to correlate these results with the states observed in EPR, since it was not made clear whether the hydrogen-reduced enzyme was predominantly in the EPR-silent reduced state or the EPR-detectable Ni-C state. EXAFS spectra of the nickel in oxidized *D. gigas* hydrogenase were best fitted with four or six sulfur atoms at a distance of 0.220 nm. Other low-atomic-number scatterers were not detected but the presence of a small number could not be ruled out.

2. *Hyperfine Interactions*

As already noted, the first application of hyperfine interactions in the EPR spectra of hydrogenase was to identify the EPR signals that are due to nickel, by using the convenient isotope ^{61}Ni. All of the signals due to nickel have been assigned in this way (Figs. 4 and 5).

The EPR spectra of oxidized hydrogenases (Fig. 4a) do not show any noticeable hyperfine splitting by ^{14}N nuclei, indicating that there is no significant delocalization onto nitrogen ligands. Neither is there any change in linewidth on exchanging H_2O by D_2O (*10, 53*).

Albracht *et al.* (54) investigated the hyperfine interaction of the nickel center with ^{33}S ligands in hydrogenase from *Wolinella succinogenes* grown in a medium enriched with the isotope. Hyperfine splitting was observed in the narrow-line EPR spectra of both oxidized hydrogenase, and the hydrogen-reduced form after illumination (cf. Fig. 5b). Although there was only partial (about 70%) isotopic enrichment, it was possible to estimate by spectral simulations the number of interacting

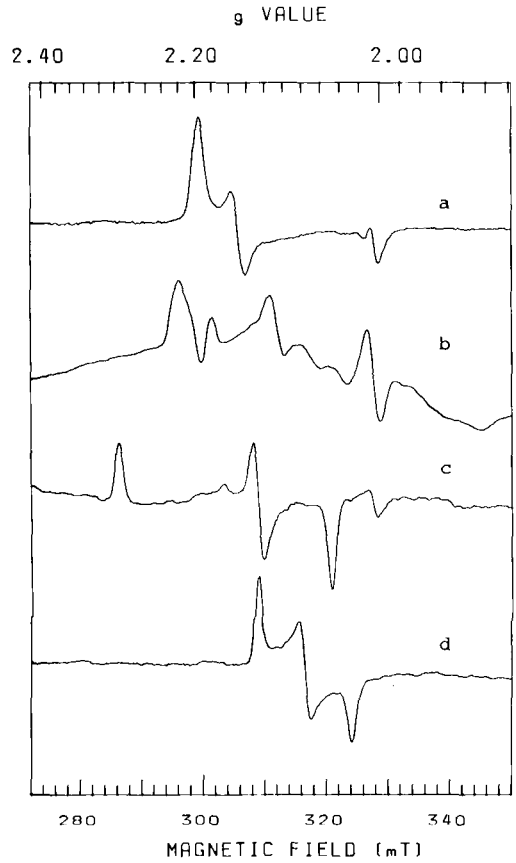

FIG. 5. EPR spectra of nickel in *D. gigas* hydrogenase: (a) Ni-C spectrum of activated hydrogenase under hydrogen, recorded at 77 K (cf. Fig. 4d); (b) same sample, recorded at 7 K, showing splitting due to interaction with reduced [4Fe–4S] cluster(s); (c) sample after illumination, recorded at 104 K; (d) hydrogen-activated hydrogenase, treated with carbon monoxide, recorded at 28 K.

sulfurs on the basis that it should be an integer value. The best fit was obtained by assuming just one interacting sulfur nucleus. The possibility cannot be discounted at present that other sulfurs are present, if the coordination geometry and electron distribution are such that the hyperfine interaction is very weak, or if the percentage enrichment of ^{33}S is overestimated. However, these results represent a significant disagreement with the estimates, from EXAFS, of three (*51*) or four (*52*) sulfurs, and further investigation is required.

The EPR spectra of Ni(III) complexes of short peptides containing thiol groups (*55*) were found to resemble those of hydrogenase most closely when they contained only one sulfur ligand. Sugiura *et al.* concluded that the most probable arrangement in hydrogenase is a single cysteine sulfur as equatorial ligand in a tetragonal geometry.

3. Electron Spin-Echo Spectroscopy

The three-pulse electron spin-echo envelope modulation (ESEEM) technique is particularly sensitive for detecting hyperfine couplings to nuclei with a weak nuclear moment, such as ^{14}N. It has been used to probe the coordination state of nickel in two hydrogenases from *M. thermoautotrophicum,* strain ΔH (*56*). One of these enzymes contains FAD and catalyzes the reduction of F_{420} (7,8-dimethyl-8-hydroxy-5-deazaflavin), while the other contains no FAD and has so far only been shown to reduce artificial redox agents such as methyl viologen.

The Fourier transform of the ESEEM spectra of the F_{420}-reducing hydrogenase showed a pattern of lines (Fig. 6b) which was interpreted as a hyperfine interaction of about 1.8 MHz with a ^{14}N nucleus (*56*). Since the spectrum was not observed in the ESEEM of the methyl viologen-reducing hydrogenase, which lacks FAD, it was suggested that the interaction might be with a flavin nitrogen. However, subsequent measurements have revealed the same interaction with nitrogen, in the hydrogenase of *Thiocapsa roseopersicina,* which contains no flavin (*101*). The magnitude of the hyperfine splitting suggests an indirect coordination of the nickel to nitrogen. It corresponds to a dipolar interaction over approximately 0.35 nm.

4. Magnetic Circular Dichroism

Magnetic circular dichroism (MCD) is a means of observing optical transitions due to paramagnetic species, and has been used by Johnson *et al.* (*57*) to observe Ni(III) against a background of iron–sulfur cluster absorption, in hydrogenases from *M. thermoautotrophicum* and *D. gigas.* Spectra of *M. thermoautotrophicum* hydrogenase were more fruitful because of the absence of paramagnetic [3Fe–xS] clusters. In the oxidized state only the nickel is paramagnetic and at low temperatures yielded MCD bands in the regions of 300–460 and 530–670 nm (Fig. 7b). These were provisionally assigned to nickel d–d transitions and sulfur-to-nickel charge transfer bands, respectively. Magnetization curves were consistent with an $S = 1/2$ ground state, as expected for low-spin Ni(III).

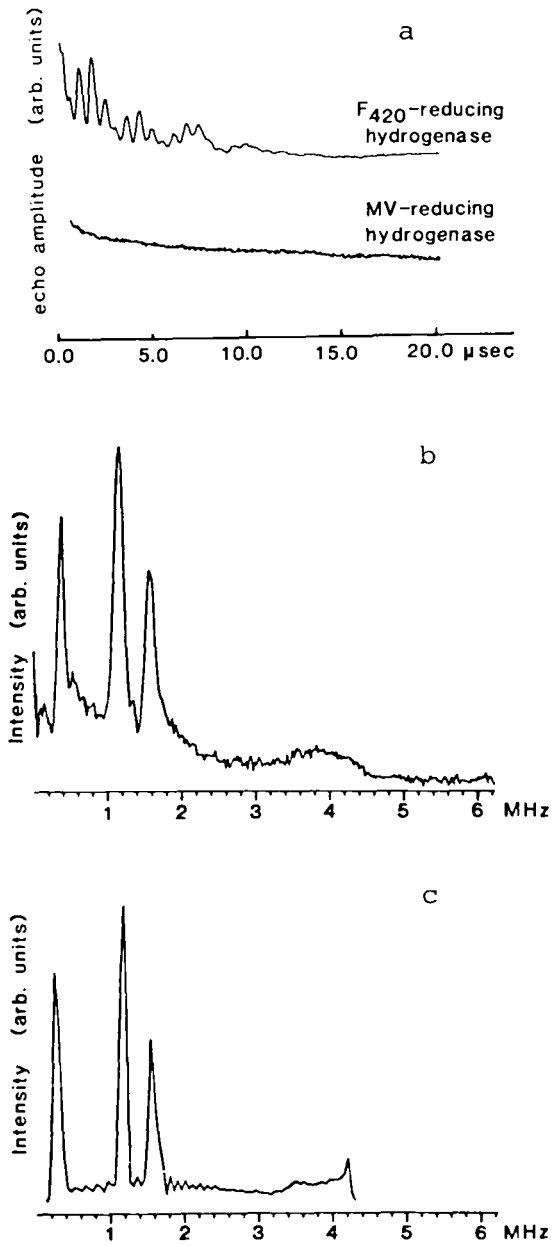

FIG. 6. ESEEM spectra of Ni in the F_{420}-reducing and methyl viologen (MV)-reducing hydrogenases from *M. thermoautotrophicum* (ΔH strain). Spectra (a) were obtained using a three-pulse stimulated-echo sequence, the time T between the second and third pulses being varied. (b) Fourier transform of FH_2ase data; (c) simulated spectra. Spectra are the average of recordings from $g = 2.0$ to 2.34. Reproduced, with permission, from Ref. *56*.

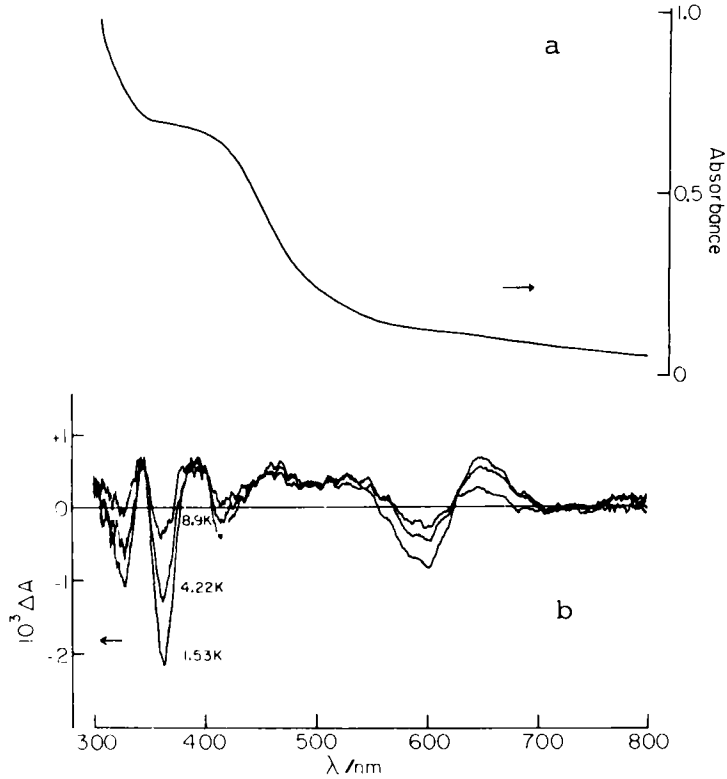

FIG. 7. Optical absorption and magnetic circular dichroism spectra of oxidized hydrogenase from *M. thermoautotrophicum* (ΔH strain), nickel concentration 120 μM. (a) Optical absorption spectrum, at room temperature; the absorption is predominantly due to iron–sulfur clusters. (b) MCD spectra recorded at 1.53, 4.22, and 8.9 K, in a magnetic field of 4.5 T; MCD is predominantly due to Ni(III), which is the only paramagnetic species in the oxidized enzyme. Reproduced, with permission, from Ref. *57*.

E. Derivatives of Nickel

Altered forms of Ni hydrogenases have been observed under conditions in which substitution is expected at the hydrogen-binding site. These have been interpreted as species containing hydrogen or hydride or carbon monoxide, respectively, and are particularly relevant to the mechanism of hydrogen production and its inhibition by carbon monoxide. So far these species have only been observed by EPR. The investigation of these species and other possible diamagnetic species by other spectroscopic techniques is awaited with interest.

1. Reactions with Hydrogen

The Ni-C EPR signal is observed in some Ni hydrogenases under hydrogen. A significant property of this nickel species is that it is photosensitive; irradiation by visible or near-ultraviolet light at cryogenic temperatures produces a new type of EPR signal (Fig. 5c). The photochemical reaction is reversed at temperatures above 200 K. The rate of photolysis was shown by Van der Zwaan *et al.* (*43*) to have a kinetic isotope effect, being nearly six times slower in D_2O than in H_2O. This indicates that the photolytic process involves displacement of a hydrogen atom in the first coordination sphere, such as a nickel hydride. If that is the case, a significant hyperfine splitting would be expected. The Ni-C signal has indeed been reported (*43, 53*) to show broadening in ^1H_2O compared with ^2H_2O (*43, 53*), though this is small (0.3–0.5 mT) considering the large magnetic moment of the ^1H nucleus.

Studies of nickel protoporphyrins by resonance Raman spectroscopy show that the photochemical behavior of nickel sites may be complex and dependent on the protein environment. Nickel, in porphyrin complexes, favors a four- or six-coordinate structure (*58*). In nickel-substituted human hemoglobin, one type of binding site takes up four-coordinate geometry (with a γ band at 406 nm), and the other type of site, like the heme-binding site in myoglobin, is forced into five-coordination (*59*). After laser excitation, the four-coordinate sites undergo photoassociation with a fifth ligand, as occurs in protoporphyrin complexes. By contrast, the five-coordinate sites undergo photodissociation (*60*). Unlike Fe porphyrins, the recombination of the displaced ligand with the nickel site is very rapid (20 p sec).

Hydrides of Ni(I) and Ni(II) are known (*37*). A Ni(II) hydride appears to be an intermediate in the catalysis of olefin isomerization by phosphine complexes of nickel (*61*). Dilworth (*62*) has pointed out that stable hydride species are not obtained in model complexes with sulfur ligands. However, they may be possible within the confines of a protein chelate.

2. Reactions with Carbon Monoxide

Carbon monoxide is an inhibitor of most nickel-containing hydrogenases, an exception being the soluble hydrogenases of hydrogen bacteria (*63*). Kinetically, inhibition is competitive with hydrogen, which indicates that the two molecules bind to the same site. EPR spectroscopy indicates that oxidized hydrogenase, giving the Ni(III) Ni-A signal, is unreactive toward carbon monoxide. Probably it is Ni(II) or Ni(I) that binds CO. Reaction of reduced hydrogenase with CO

produces both EPR-silent and EPR-detectable (Fig. 5d) states, which may represent different carbonyl species (*64, 65*).

The EPR-detectable CO derivative in *C. vinosum* hydrogenase was shown by Van der Zwaan *et al.* (*64*) to be photolysed at low temperatures, yielding a product having the same spectrum as the photolyzed hydrogen-treated enzyme (Fig. 5c). Unlike the hydrogen-reduced species however, the rate of photolysis was unaffected by deuterium isotope substitution.

3. Interactions with Oxygen

Oxygen is inhibitory toward some hydrogenases and completely destructive toward others, particularly some Fe hydrogenases (*66*). In those hydrogenases which can survive exposure to oxygen, the hydrogenase active site is unreactive toward H_2 and CO under oxidizing conditions (not necessarily the presence of oxygen). In *D. gigas* hydrogenase, DerVartanian *et al.* (*53*) have noted an increase in the spin-lattice relaxation rate of the Ni-A EPR signal under oxygen, consistent with an interaction with the triplet state of O_2. This has been interpreted (*74*) as the binding of oxygen to the nickel site, but, at present, the evidence for this is not conclusive, since the lineshape of the Ni-A signal did not change. If oxygen is associated with the Ni-A site, it must be extremely tenaciously bound, since the enzyme is unaffected by stringent removal of dissolved oxygen (*49*). It seems more likely that there is a protective mechanism for those organisms which may encounter oxygen *in vivo*, whereby the hydrogenase active site becomes inaccessible to all gases. A similar type of oxidative stabilization and reductive reactivation is observed in the Fe hydrogenase of *Desulfovibrio vulgaris* (Hildenborough strain) (*67*). It is therefore possible that the ability to form such a state depends upon some specific structure within the enzyme molecule which is distinct from the hydrogen-binding site.

F. Interactions of Nickel with Iron–Sulfur Centers

All the hydrogenases which have been isolated are iron–sulfur proteins. In particular, hydrogenase activity seems to be associated with at least one [4Fe–4S] cluster in addition to nickel. In some hydrogenases, including the catalytic dimer of *N. opaca* hydrogenase, both the iron–sulfur cluster and the nickel are undetectable by EPR, and it is possible that in these cases there is strong antiferromagnetic coupling. The two groups might act together to transfer two electrons to hydrogen.

Many of the Ni hydrogenases contain an iron–sulfur cluster presumed to be of the [3Fe–xS] type, which is paramagnetic with S = 1/2 in the oxidized state and $S = 2$ in the reduced state (*68, 69*). The function of these clusters is unknown. In some hydrogenases, typified by *C. vinosum* hydrogenase and the membrane-bound hydrogenase of *Alcaligenes eutrophus* (*70*), the EPR spectra of the iron–sulfur cluster and the oxidized nickel center show complex lineshapes (Fig. 8). In *C. vinosum* the nickel is also EPR detectable and its spectrum also shows

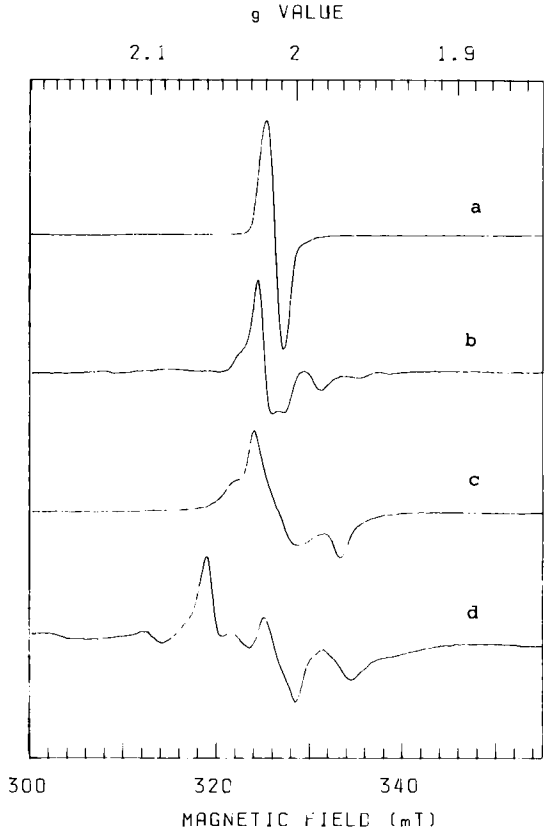

FIG. 8. EPR spectra of [3Fe–xS] clusters in oxidized hydrogenases, showing the influences of weak Ni–Fe–S electron-spin interactions. (a) *Desulfovibrio desulfuricans* (strain Norway 4) hydrogenase, showing the spectrum of an isolated [3Fe–xS] cluster; (b) *Chromatium vinosum* hydrogenase; the outer lines (Signal 2) correspond to interaction with Ni(III); (c) *Paracoccus denitrificans* hydrogenase; (d) *Alcaligenes eutrophus* membrane-bound hydrogenase. Spectra were recorded at approximately 20 K. Samples were provided by K. K. Rao, J. Serra, and K. Schneider.

splitting at temperatures where the iron–sulfur cluster is detectable (*71*). Spectra recorded at *S*-band and *Q*-band frequencies confirmed that these effects were due to spin–spin interaction presumably between the nickel and iron–sulfur clusters (*71*).

In *D. gigas* hydrogenase, splittings are not observed in the Ni-A and Ni-B signals from oxidized nickel centers (Fig. 4a), but are seen in the reduced Ni-C species at low temperatures (Fig. 5b) (*41, 72*). The splitting of Ni-C correlates with the reduced state of a [4Fe–4S] cluster (*72*). The spin–spin interactions observed in EPR are consistent with a distance between the nickel and iron-sulfur cluster of less than 1.2 nm (*73*).

G. Catalytic Properties

1. Activity States of Nickel-Containing Hydrogenases

The characteristic EPR signal due to Ni(III) (Fig. 4a) is observed in a number of hydrogenases, but not all (*14, 15*). This is consistent with the view that the signal reflects an oxidized form of the enzyme which is not directly involved in catalysis. This is supported by studies of the enzyme activity in response to oxidizing and reducing agents. A well-studied case is that of hydrogenase from *D. gigas* (*41, 49*). Even when extensive precautions are taken to remove oxygen, a reductant is still necessary to reduce the oxidized hydrogenase to a state which is capable of reacting with hydrogen (*69*).

The enzymatic activity of hydrogenases, whether measured by hydrogen production, hydrogen consumption, or hydrogen isotope exchange, is often variable, depending on the history of the sample. The hydrogenases may not manifest their full activity until they have been subjected to reactivating treatments, which vary from one hydrogenase to another. For instance, *D. gigas* hydrogenase shows a phenomenon of slow activation by hydrogen or other strong reductants (*74, 75*). A study of the conditions required for the slow activation of *D. gigas* hydrogenase showed that it was not induced by addition of chelating agents, or nickel ions, or reagents which in other systems have caused the conversion of [3Fe–*x*S] clusters to [4Fe–4S] (*49*). The thiol-reducing agent dithiothreitol (DTT) did not cause activation when added alone [although in certain circumstances it can have an activating effect on *C. vinosum* hydrogenase (*76*)]. The changes in activity of *D. gigas* hydrogenase when incubated under hydrogen are illustrated in Fig. 9a, and EPR spectra of the nickel in the enzyme are shown in Fig. 9b. The fact that the enzyme can be obtained in forms with different activity, which can all be fully reactivated, indicates that there must be more

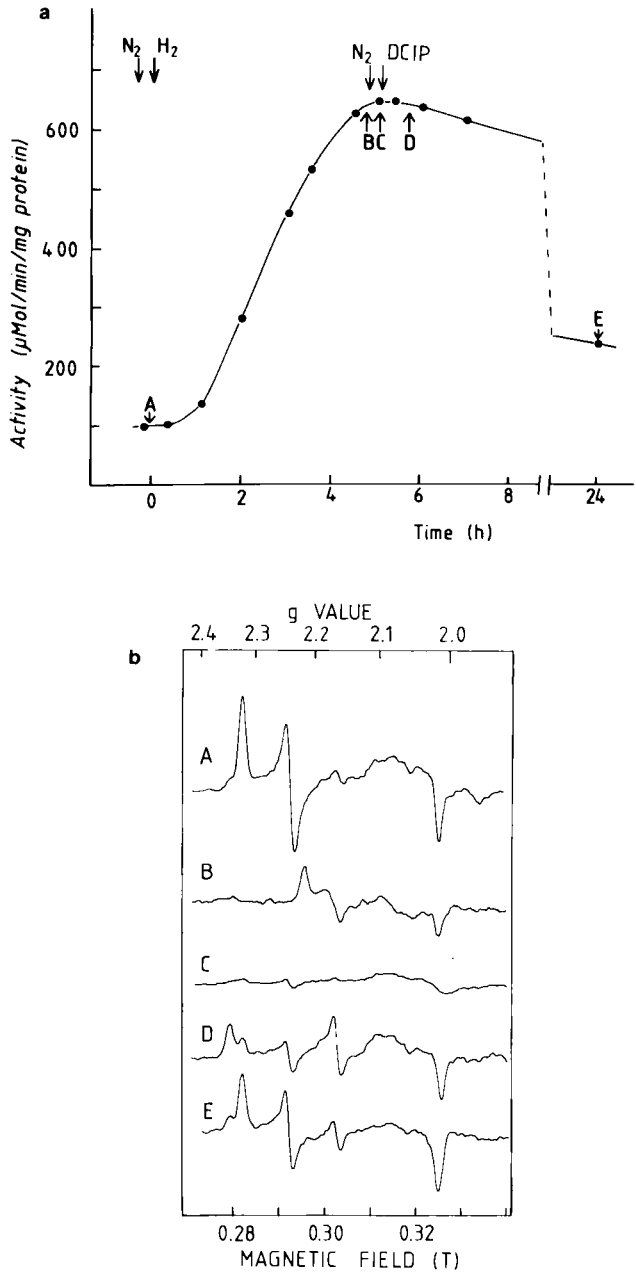

FIG. 9. (a) Activity of *D. gigas* hydrogenase (hydrogen–methyl viologen reductase) during activation under hydrogen, flushing with nitrogen, and reoxidation with dichloroindophenol (DCIP). (b) EPR spectra of samples taken at points A–E, as indicated in a, recorded at 80 K. See text for details. Adapted from Refs. *40* and *49*.

than one type of inactive oxidized enzyme. The simplest hypothesis is that there are two: one which is activated rapidly by reduction during the assay, and one which is only activated slowly by strong reductants. We have termed these forms the *ready* and *unready* states, respectively, of the enzyme. The catalytic and spectroscopic properties of the enzyme in these states are described in Table III. In the interpretation of Berlier *et al.* (*74*), the unready state is associated with a tightly bound oxygen molecule. Alternatively, the ready and unready states might represent different protein conformations (*49*).

The enzyme, which had been prepared in the presence of air (marked point A in Fig. 9a), is mostly in a state which has been described as *unready* (*49*). It has an activity, which corresponds to about 12% of the *active* state, in hydrogen uptake with methyl viologen, but is completely inactive in hydrogen isotope exchange (*74, 77*) or hydrogen uptake with a high-potential acceptor dye such as 2,6-dichloroindophenol (DCIP). We proposed that the enzyme at this stage consists of about 88% of the *unready* and 12% of the *ready* state.

After complete activation under hydrogen, a process which requires about 4 hours at 20°C (point B), the hydrogenase is fully active in all assays (*49, 74*). If hydrogen is then removed and the enzyme reoxidized with the dye dichloroindophenol at pH 7.8, the enzyme is principally in the *ready* state (point C), which is fully active in the hydrogen–methyl viologen reductase assay, but completely inactive in hydrogen isotope exchange (*77*), and is stable in air for several hours. This observation particularly indicates that the appearance or loss of activity of the enzyme is not entirely due to the removal or addition of oxygen. The

TABLE III

ACTIVITY STATES OF *D. gigas* HYDROGENASE[a]

	State		
Activity	Active	Ready	Unready
H_2–methyl viologen	Active	Active after lag	Inactive
H_2–DCIP	Active	Inactive	Inactive
H_2–isotope exchange	Active	Inactive	Inactive
Hydrogen production	Active	Active	Inactive
		EPR signals	
	Ni-C	Ni-B	Ni-A
	Broad $[4Fe-4S]_{red}$	$[3Fe-xS]_{ox}$	$[3Fe-xS]_{ox}$

[a] Conditions of formation: active state incubation under H_2, ready state anaerobic oxidation, unready state oxygen or strong reductants by DCIP, pH 8.0.

EPR signal at this stage corresponds mainly with the Ni-B signal (Figs. 4d and 5a), which was therefore proposed to represent the *ready* state (*40*). After prolonged exposure to oxygen, the enzyme reverts to the *unready* state and the Ni-A signal reappears (point E).

Hydrogenases differ greatly in the rate and extent of reductive activation (*14*); *D. gigas* appears to represent a slow extreme. In other hydrogenases, such as the soluble enzymes from hydrogen bacteria, the reductive activation is always too rapid to be measurable. These hydrogenases also differ from *D. gigas* hydrogenase in that they give no Ni(III) signal in their oxidized states, and give different HD/H_2 ratios in the isotope-exchange reaction (*78*). It is not not known if these factors are correlated.

Another pattern of reductive activation has been observed in the Ni hydrogenase of *Methanobacterium formicicum* (*79*). In this enzyme, reductive activation is irreversible, requires a strong reductant, and is inhibited by the chelating agent 2,2′-bipyridyl. The conversion of a [3Fe–xS] cluster to a [4Fe–4S] has been suggested.

2. *Mechanism of Catalysis*

The behavior of the EPR-detectable nickel and iron–sulfur species in hydrogenase during redox-poising experiments suggests several possible reaction sequences. The Ni-C species is particularly significant since the potentials for its appearance and subsequent disappearance during reduction are comparable with the H^+/H_2 potential, at the low partial pressures of hydrogen likely to be encountered by these organisms; the potentials are also pH dependent, consistent with hydrogen production. Moreover, the low-temperature photochemical reaction of the Ni-C species shows a strong kinetic isotope effect with ^2H.

The series of steps of reduction have been variously interpreted:

Ni(II)	= Ni(I)	= Ni(O)	(*43*)	(1)
EPR silent	Ni-C signal	EPR silent		
Ni(III)–[4Fe–4S]$^-$	= Ni(III)·H$^-$	= Ni(II)	(*41*)	(2)
Ni(II)	= Ni(I)	= Ni(II)·H$^-$	(*72*)	(3)

It is difficult to distinguish these possibilities on the basis of the EPR spectra since the spectra of low-spin d^7 Ni(III) and d^9 Ni(I) are similar. A disadvantage of Scheme (1) is that it requires the nickel to take up oxidation states from Ni(III) to Ni(O) over a potential range of about 240 mV, whereas in inorganic complexes they span several volts (*80*). In Scheme (2) (*41*), the nickel is coupled to an iron–sulfur cluster. On

reduction of the oxidized hydrogenase, the disappearance of the Ni-A Ni(III) signal is due to reduction of the iron–sulfur cluster, which becomes paramagnetic on reduction, giving net zero spin; however, optical absorption changes on reduction of *D. gigas* hydrogenase do not support this view (*40*). Scheme (3) was proposed to explain why only a very small ^1H hyperfine splitting is seen in the Ni-C species, whereas a stronger coupling would be expected for a paramagnetic nickel hydride (*72*).

The hypothetical reaction mechanism shown in Fig. 10 is a variation of Scheme (3), and is consistent with the redox and pH dependence of the EPR-detectable nickel species (*65*). Hydrogen is known to undergo heterolytic cleavage (*81*); it is proposed that this is an intramolecular reaction, leading to the formation of a nickel (II) hydride and a protonated base in the enzyme (Step 1 in Fig. 10). The Ni-C species is postulated to be a protonated Ni(I) species. An alternative formulation for this state would be a dihydrogen complex, $Ni(III)\cdot H_2$, as suggested by Crabtree (*104*). Ultimately the exact mechanism can only be determined by kinetic measurements.

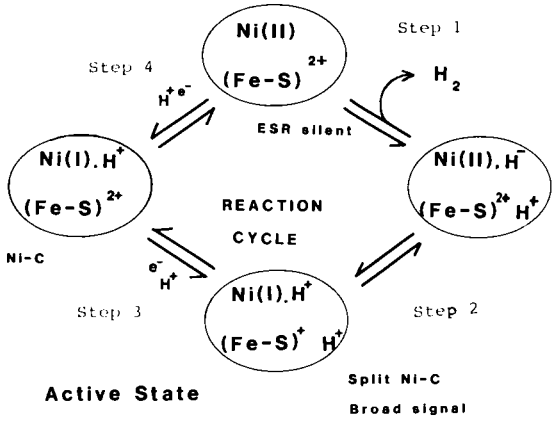

FIG. 10. Hypothetical reaction cycle for *D. gigas* hydrogenase, based on the EPR and redox properties of the nickel (Table II). Only the nickel center and one [4Fe–4S] cluster are shown. Step 1: enzyme, in the activated conformation and Ni(II) oxidation state, causes heterolytic cleavage of H_2 to produce a Ni(II) hydride and a proton which might be associated with a ligand to the nickel or another base in the vicinity of the metal site. Step 2: intramolecular electron transfer to the iron–sulfur cluster produces a protonated Ni(I) site (giving the Ni-C signal). An alternative formulation of this species would be $Ni(III)\cdot H_2$. Step 3: reoxidation of the iron–sulfur cluster and release of a proton. Step 4: reoxidation of Ni and release of the other proton.

H. Other Functions of Nickel in Hydrogenases

The soluble hydrogenase from the hydrogen-oxidizing bacterium *N. opaca* is one of a class of hydrogenases that contain flavin and use nicotinamide adenine dinucleotide (NAD) as electron acceptor. The protein consists of four dissimilar subunits and contains approximately four atoms of nickel, one FMN, three [Fe–4S] clusters, one [2Fe–2S] cluster, and up to one [3Fe–xS] cluster (*82*). Two of the nickel atoms were readily removed by dialysis, in contrast to the nickel in most hydrogenases. The enzyme would only catalyze electron transfer from hydrogen to NAD if cations, of which Ni^{2+} is the most effective, were added. In the absence of the cations, the enzyme could be separated as

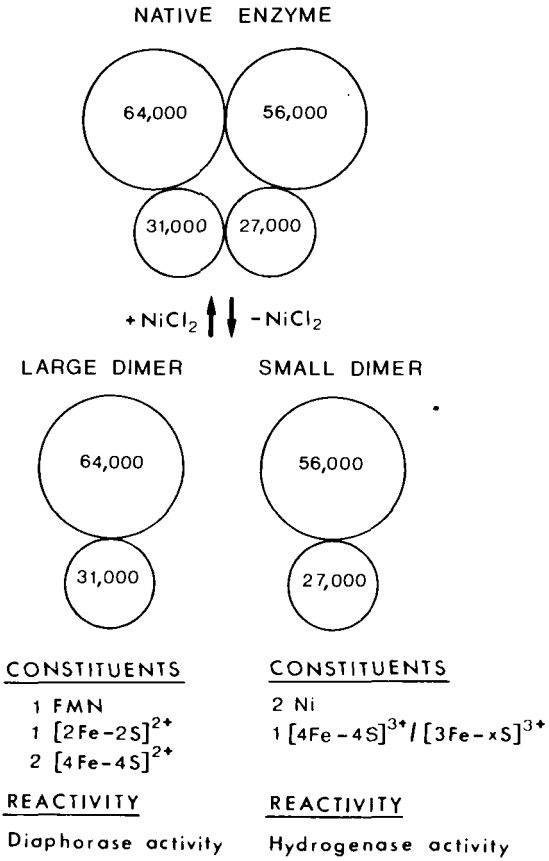

FIG. 11. Dissociation and reassociation of soluble, NAD-linked hydrogenase from *Nocardia opaca*. "Diaphorase" refers to NADH : acceptor reductase activity. Reproduced, with permission, from Ref. *82*.

two dimers (Fig. 11). One of these contained two tightly bound nickel atoms and one [4Fe–4S] cluster, and had hydrogen:acceptor reductase activity. The other contained flavin and iron–sulfur clusters and had NADH:acceptor reductase activity. Hence in *N. opaca* hydrogenase, which so far is a unique case, the nickel has two functions, in catalysis and in maintaining protein structure.

IV. Methyl-Coenzyme M Reductase

A. Factor 430

F_{430}, a yellow, water-soluble compound, was first extracted from boiled cells of methanogenic bacteria, a discovery which Wolfe (*19*) has credited to J. LeGall. Its isolation was first reported by Gunsalus and Wolfe (*83*). The cofactor has a Soret band in the visible region at 430 nm. Functionally F_{430} is a prosthetic group of the methylreductase system (*24, 84*). It is also found in the free state in cell extracts (*85*).

The presence of nickel in F_{430} was demonstrated by Diekert *et al.* (*86*) and Whitman and Wolfe (*87*). Biosynthetic incorporation of δ-aminolevulinic acid indicated that the compound has a tetrapyrrole structure. The structure of the methanolysis product of F_{430} was determined by Pfaltz *et al.* (*88*) using NMR spectroscopy. The structure of the cofactor in the cell is probably the penta acid (Fig. 12). It is a tetrahydro derivative of a porphinoid which is related to the corrins, for which Pfaltz *et al.* (*88*) have coined the term "corphin." Specificity of this macrocycle for nickel is afforded by the six-membered ring, which introduces a slight pucker into the planar structure. EXAFS measurement of the nickel environment of isolated F_{430} indicated two nitrogens at 0.191–0.192 and 0.210–0.214 nm (*89a, 89b*). This is consistent with nickel in a square–planar coordination to a puckered corphin structure. In the intact protein, protein component C of methyl-CoM reductase, the absorption-edge spectra are indicative of nickel with a coordination number greater than four, probably octahedral (*89c*).

B. EPR Spectra

Albracht *et al.* (*90*) have observed an EPR spectrum from whole cells of *M. thermoautotrophicum* (Fig. 13) which appears to arise from protein-bound F_{430}. The same type of spectrum was also observed in purified methyl-CoM reductase. The paramagnetic species on whole cells was only partially reduced by treatment with hydrogen and was unaffected by carbon monoxide. Gel filtration showed it to be part of a soluble protein. The spectrum was somewhat broadened by substitution

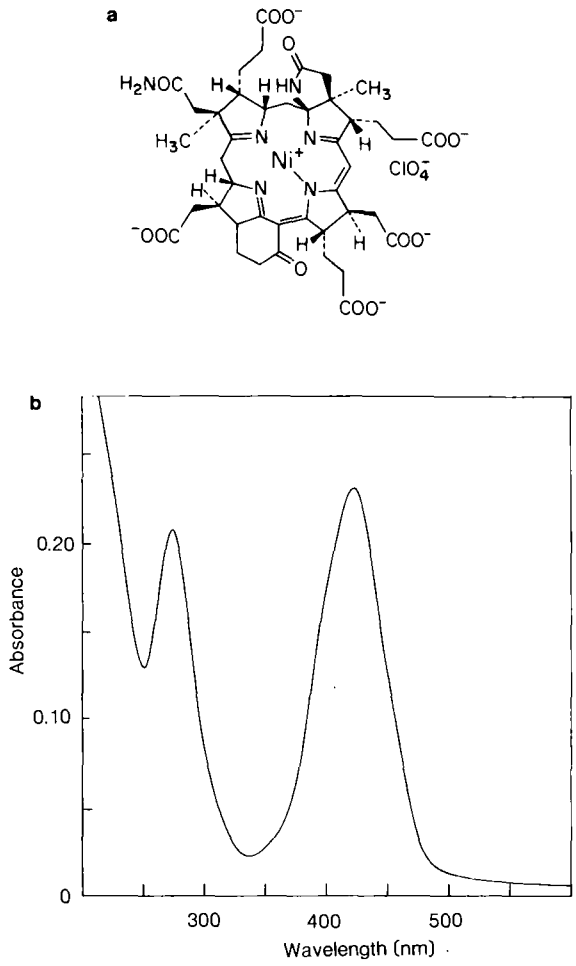

FIG. 12. (a) Structure of F_{430}, deduced from the structure of the methanolysis product (88). (b) UV/visible absorption spectrum of F_{430} in water, concentration $10^{-5}M$.

with ^{61}Ni and showed hyperfine splitting which could be simulated as interaction with four equivalent nitrogen atoms, corresponding to the *four nitrogens of a tetrapyrrole. The lineshape of the spectrum is consistent with nickel in a tetragonally distorted octahedral ligand field.* This confirms the assignment as a nickel species bound in a planar tetrapyrrole structure. It was not possible to determine the oxidation state of the nickel, although the observation that it was observed in isolated factor F_{430} treated with dithionite suggests that it is Ni(I).

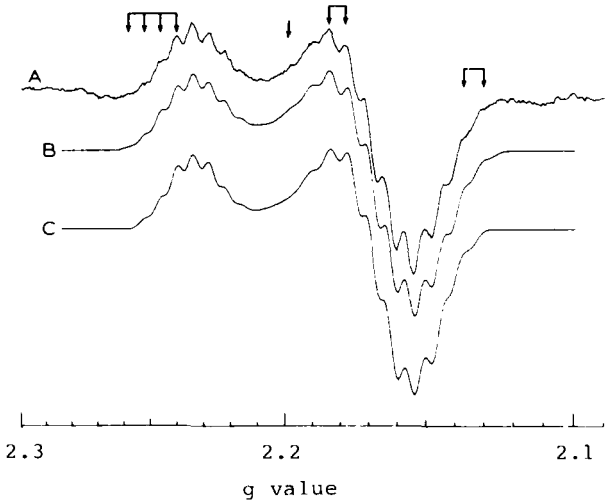

FIG. 13. (A) EPR spectrum, recorded at 70 K, of reduced F_{430}, in a hydrogen-reduced cell extract from *M. thermoautotrophicum* (Marburg strain). (B and C) Computer simulations, assuming equal interaction with four (B) or three (C) equivalent ^{14}N nuclei. The arrows indicate places where B gives a better fit. Reproduced, with permission, from Ref. *90*.

C. FUNCTION

F_{430} is required for the activity of the methylreductase system, which catalyzes the reduction of the methyl group of methyl-CoM, i.e., 2-(methylthio)ethanesulfonate, to methane:

$$CH_3—S—CH_2—CH_2—SO_3^- + H_2 \longrightarrow CH_4 + HS—CH_2—CH_2—SO_3^- \quad (4)$$

This is a complex process, involving the deazaflavin-reducing hydrogenase and other proteins, provisionally named factors A-2, A-3, and C (*19*). The system requires initial activation by ATP before the reaction can proceed (*87*). Component C consists of two each of three protein subunits of 68, 45, and 38.5 kDa and contains two molecules of F_{430} per molecule, as well as stoichiometric amounts of coenzyme M (*91*). F_{430} appears to be tightly but noncovalently bound to the enzyme.

The exact role of the nickel of F_{430} in methane formation is not clear at present. Analogy with the cobalamins, and the observation of an EPR-detectable reduced state, might suggest that it is involved in either methyl group transfer, reduction, or both.

V. Carbon Monoxide Oxidoreductase

A. Catalytic Properties

Carbon monoxide oxidoreductase (carbon monoxide dehydrogenase) catalyzes the interconversion of CO and CO_2 with suitable electron acceptors and donors. The reaction takes place via an enzyme-bound one-carbon intermediate:

$$CO \longrightarrow [C_1] \longrightarrow CO_2 + 2e^- + 2H^+ \quad (5)$$

The enzyme was first isolated from *C. thermoaceticum*, *Clostridium formicoaceticum*, and *Clostridium pasteurianum* by Diekert and Thauer (*92*), who demonstrated that synthesis of the enzyme requires nickel (*93*). The enzyme is present in large amounts in acetogenic bacteria, where it is involved in an unusual pathway for fixation of CO_2 with the formation of acetate (*25, 26*). In acetogens this reaction is involved both in production of energy, with acetate as a waste product, and in biosynthesis of cell constituents starting from acetate. CO oxidoreductase is also present in methanogenic bacteria, where it is used in biosynthetic metabolism (*25, 27*).

Other reactions catalyzed by CO oxidoreductase, which may be more relevant to its physiological function, are the exchange between CO and the carbonyl group of acetyl-CoA (*94*)

$$CH_3—*CO—CoA + CO \longrightarrow CH_3—CO—CoA + *CO \quad (6)$$

and the exchange between CoA and the CoA moiety of acetyl-CoA.

$$CH_3—CO—S*CoA + CoASH \longrightarrow CH_3—CO—CoA + *CoASH \quad (7)$$

The reaction [Eq. (7)] requires a disulfide-reducing system such as dithiothreitol or disulfide reductase and a reducing agent such as NADPH or reduced ferredoxin. It is proposed [Eq. (5)] that carbon monoxide oxidoreductase binds CO as a one-carbon intermediate [C_1], which can be either oxidized to CO_2 or condensed with the methyl group of a methylated corrinoid protein and CoA in the final step of acetyl-CoA synthesis.

Carbon monoxide oxidoreductase has a high molecular weight; values between 150,000 and 460,000 have been reported (*25*). Analysis of the enzyme from *C. thermoaceticum* indicated a composition of 2 atoms of Ni, 1 Zn, 11 Fe, and 14 inorganic sulfide per dimeric enzyme, with a relative molecular mass of approximately 150,000 Da (*23*).

B. Spectroscopy

Low-temperature EPR spectroscopy of carbon monoxide oxidoreductase in the reduced state gave a complex spectrum with g values 2.04, 1.94, and 1.90, and 2.01, 1.86, and 1.75, which probably represent two [4Fe–4S] clusters (*95*). The clusters are oxidized by CO_2 and reduced by CO.

EPR spectra of CO oxidoreductase under non reducing conditions showed a spectrum at $g = 2.21$, 2.11, and 2.02, which, by analogy with spectra observed in nickel-containing hydrogenases, was attributed to Ni(III) (*96*). The spectrum was of low intensity and it was not established whether it represents an active state of the enzyme.

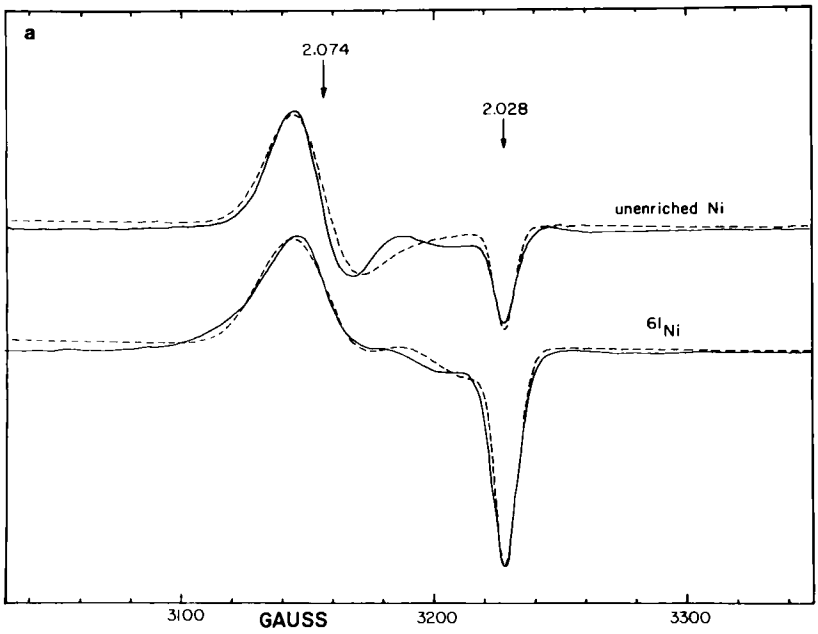

FIG. 14. EPR spectra of carbon monoxide oxidoreductase from *C. thermoaceticum*, treated with CO plus coenzyme A. Solid lines are experimental spectra, dashed lines are computer simulations, with $g_x = g_y = 2.074$, $g_z = 2.028$. Substitutions with ^{61}Ni and ^{57}Fe were made by growth of the organism on the appropriate isotopes. (a) Effect of substitution with ^{61}Ni. Simulation assumes $A_{||} = 3$ MHz, $A_{\perp} = 20$ MHz. (b, p. 328) Effects of substitution with ^{57}Fe and ^{13}C. The simulation of the ^{57}Fe spectrum assumes one iron atom with $A_{||} = 40$ MHz, $A_{\perp} = 60$ MHz, and two iron atoms with $A_{||} = 20$ MHz, $A_{\perp} = 30$ MHz. The simulation of the ^{13}C spectrum assumes $A_{||} = 26$ MHz, $A_{\perp} = 13$ MHz. Spectra provided by courtesy of Dr. S. G. Ragsdale.

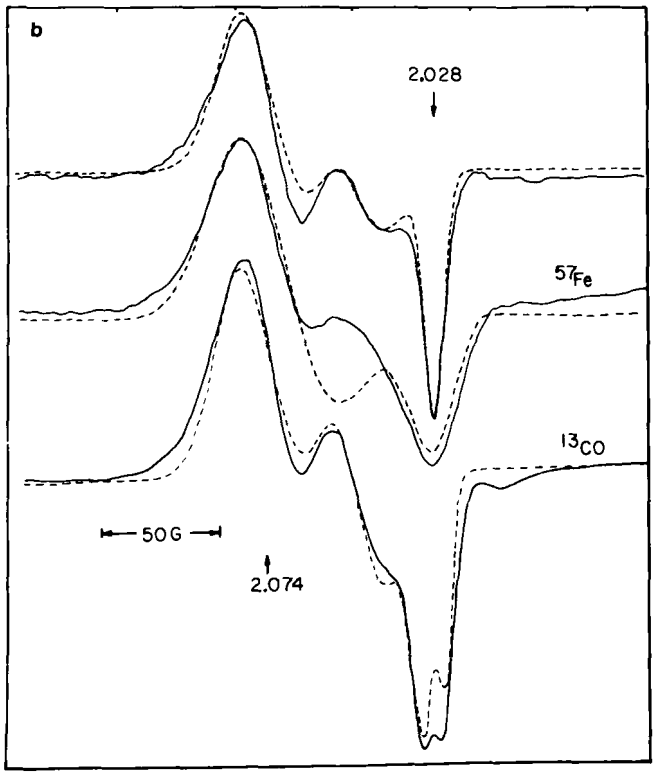

FIG. 14b. See legend on p. 327.

Two spectra which are more clearly relevant to the enzyme-catalyzed reaction were observed in the reduced enzyme after treatment with CO (Fig. 14). A rhombic spectrum, Signal 2, with g values of 2.062, 2.047, and 2.028, was observed upon reaction of carbon monoxide oxidoreductase with CO (*97*). Addition of coenzyme A or acetyl-CoA induced an axially symmetric spectrum, Signal 1, at $g = 2.074$ and 2.028. Spectra of the CO-treated carbon monoxide oxidoreductase were typically a mixture of the two species. It was assumed that these spectra represent different enzyme–C_1 intermediates. The spectrum showed hyperfine broadening after reaction with ^{13}CO instead of ^{12}CO and in enzyme from cells grown on ^{61}Ni (*96*). Subsequently it was shown (*97*) that the spectrum was broadened by substitution of ^{57}Fe (Fig. 14). These results demonstrated that the radical species is a complex containing nickel, carbon monoxide, and iron. Recent simulations (*103*) show that the spectra are consistent with a complex of one nickel and three iron atoms, analogous to a [4Fe–4S] cluster in which one iron atom is substituted by nickel.

This represents a new and fascinating type of mixed-metal cluster in biochemistry.

VI. Concluding Remarks

The four types of nickel-containing enzymes are quite distinct in the coordination sites and catalytic function of the nickel centers. In urease, the nickel appears to be bound to oxygen and nitrogen ligands and appears to remain as Ni(II), a state which favors octahedral or square–planar coordination. The function of nickel in this unique case may be analogous to that of zinc in other hydrolases such as carboxypeptidase.

In all the other nickel enzymes, there is scope for redox reactions at the nickel site, though it has not been demonstrated in all cases. The nickel in hydrogenase shows indications of at least one sulfur ligand, the others probably being oxygen; the ease with which oxidation states Ni(III) and, possibly, Ni(I) can be achieved indicates that the geometry might be distorted toward tetrahedral. In methyl-CoM reductase the nickel is held by a novel type of porphinoid macrocycle which is almost planar. In the protein, the geometry is presumably octahedral. The nickel may be capable of achieving the oxidation states Ni(II) and Ni(I). Finally, in CO oxidoreductase, hyperfine interactions suggest a mixed Ni–Fe cluster which is capable of binding a one-carbon group. The chemistry of the latter is probably the most fascinating and the least understood at present.

VII. Abbreviations

CoA, Coenzyme A
CoM, Coenzyme M

DCIP, 2,6-Dichloroindophenol

EPR, Electron paramagnetic resonance
ESEEM, Electron spin-echo envelope modulation
EXAFS, Extended X-ray absorption fine structure

FAD, Flavin adenine dinucleotide

MCD, Magnetic circular dichroism

NAD, Nicotinamide adenine dinucleotide
NADP, Nicotinamide adenine dinucleotide phosphate

References

1. Dixon, N. E., Gazzola, C., Blakeley, R. L., and Zerner, B., *J. Am. Chem. Soc.* **97,** 4131 (1975).
2. Sumner, J. B., *J. Biol. Chem.* **69,** 435 (1926).
3. Klucas, R. V., Hanus, F. J., Russell, S. A., and Evans, H. J., *Proc. Natl. Acad. Sci. U.S.A.* **86,** 2253 (1983).
4. Eskew, D. L., Welch, R. M., and Cary, E. E., *Science* **222,** 621 (1983); Eskew, D. L., Welch, R. M., and Norvell, W. A., *Plant Physiol.* **76,** 691 (1984).
5. Thauer, R. K., Diekert, G., and Schönheit, P., *Trends Biochem. Sci.* **11,** 304 (1980).
6. Balch, W. E., Fox, G. E., Magrum, L. J., Woese, C. R., and Wolfe, R. S., *Microbiol. Rev.* **43,** 260 (1979).
7. Lancaster, J. R., Jr., *FEBS Lett.* **115,** 285 (1980).
8. Lancaster, J. R., Jr., *In* "Methods in Enzymology" (S. Fleischer and L. Packer, eds.), Vol. 54, p. 412. Academic Press, New York, 1982.
9. Albracht, S. P. J., Graf. E.-G., and Thauer, R. K., *FEBS Lett.* **140,** 311 (1982).
10. Cammack, R., Patil, D., Aguirre, R., and Hatchikian, E. C., *FEBS Lett.* **142,** 289 (1982).
11. LeGall, J., Ljungdahl, P. O., Moura, I., Peck, H. D., Xavier, A., Moura, J. J. G., Teixeira, M., Huynh, B. H., and DerVartanian, D. V., *Biochem. Biophys. Res. Commun.* **106,** 610 (1982).
12. Albracht, S. P. J., Kalkman, M. L., and Slater, E. C., *Biochim. Biophys. Acta* **724,** 309 (1983).
13. Schneider, K., Patil, D. S., and Cammack, R., *Biochim. Biophys. Acta* **748,** 353 (1983).
14. Cammack, R., Fernandez, V. M., and Schneider, K., *Biochimie* **68,** 85 (1986).
15. Cammack, R., Hall, D. O., and Rao, K. K., *In* "Microbial Gas Metabolism: Mechanistic, Metabolic and Biotechnological Aspects" (R. K. Poole and C. S. Dow, eds.), p. 209, Academic Press, London, 1985.
16. Cammack, R., Fernandez, V. M., and Schneider, K., *In* "Bioinorganic Chemistry of Nickel" (J. R. Lancaster, Jr., ed.); VCH Publ., Deerfield Beach, Florida, 1988 (in press).
17. Bagyinka, C., and Kovacs, K., *Biochimie* **68,** pp. 1–221 (1986).
18. Lancaster, J. R. Jr., "Bioinorganic Chemistry of Nickel" (J. R. Lancaster, Jr., ed.). VCH Publ., Deerfield Beach, Florida, 1987 (in press).
19. Wolfe, R. S., *Trends Biochem. Sci.* **16,** 306 (1985).
20. Thauer, R. K., *Biol. Chem. Hoppe-Seyler* **366,** 103 (1985).
21. Keltjens, J. T., and Van der Drift, C., *Microbiol. Rev.* **39,** 259 (1986).
22. Woese, C. R., Magrum, L. J., and Fox, G. E., *J. Mol. Evol.* **11,** 245 (1978).
23. Ragsdale, S. G., Clark, J. E., Ljungdahl, L. G., Lundie, L. L., and Drake, H. L., *J. Biol. Chem.* **258,** 2364 (1983).
24. Diekert, G., Fuchs, G., and Thauer, R. K., *In* "Microbial Gas Metabolism: Mechanistic, Metabolic and Biotechnological Aspects" (R. K. Poole, and C. S. Dow, eds.), p. 115 Academic Press, London, 1985.
25. Zeikus, J. G., Kerby, R., and Krzycki, J. A., *Science* **227,** 1167 (1985).
26. Hemming, A., and Blotevogel, K. H., *Trends Biochem, Sci.* **16,** 198 (1985).
27. Fuchs, G., *FEMS Microbiol. Rev.* **39,** 181 (1986).
28a. Adams, M. W. W., and Mortenson, L. E., *J. Biol. Chem.* **259,** 7045 (1984).
28b. Huynh, B. H., Czechowski, M. H., Krüger, H. J., DerVartanian, D. V., Peck, H. D., and LeGall, J., *Proc. Natl. Acad. Sci. U.S.A.* **81,** 3728 (1984).
29. Hausinger, R. P., *Microbiol. Rev.* **51,** 22 (1987).
30a. Sunderman, F. W., Jr. *et al.* (eds.), "Nickel in the Human Environment." Scientific Publications, Lyon, France, 1984.

30b. Brown, S. S., and Sunderman, F. W., Jr., *Proc. Int. Congr. Nickel Metab. Toxicol. 3rd, Paris* (1985).
31. Blakeley, R. L., Dixon, N. E., and Zerner, B., *Biochim. Biophys. Acta* **744,** 219 (1983).
32. Rosenberg, R. C., Root, C. A., and Gray, H. B., *J. Am. Chem. Soc.* **97,** 21 (1975).
32a. Rees, D. C., Howard, J. B., Chakrabarti, P., Yeates, T., Hsu, B. T., Hardman, K. D., and Lipscomb, W. N., *In* "Zinc Enzymes" (I. Bertini, C. Luchinat, W. Maret, and M. Zeppezauer, eds.), p. 155. Birkhäuser Verlag, Boston, 1986.
33. Hasnain, S. S., and Piggott, B., *Biochem. Biophys. Res. Commun.* **112,** 279 (1983).
34. Alagna, L., Hasnain, S. S., Piggott, B., and Williams, D. J., *Biochem. J.* **220,** 591 (1984).
35. Dixon, N. E., Riddles, P. W., Gazzola, C., Blakeley, R. L., and Zerner, B., *Can. J. Biochem.* **58,** 1335 (1980).
36. Spratt, T. E., Sugimoto, T., and Kaiser, E. T., *J. Am. Chem. Soc.* **105,** 3679 (1983).
37. Nag, K., and Chakravorty, A., *Coord. Chem. Rev.* **33,** 87 (1980).
38. Hornhardt. S., Schneider, K., and Schlegel, H. G., *Biochimie* **68,** 15 (1986).
39. Kojima, N., Fox, J. A., Hausinger, R. P., Daniels, L., Orme-Johnson, W. H., and Walsh, C., *Proc. Natl. Acad. Sci. U.S.A.* **80,** 378 (1983).
40. Fernandez, V. M., Hatchikian, E. C., Patil, D. S., and Cammack, R., *Biochim. Biophys. Acta* **883,** 145 (1986).
41. Teixeira, M., Moura, I., Xavier, A. V., Huynh, B. H., DerVartanian, D. V., Peck, H. D., Jr., LeGall, J., and Moura, J. J. G., *J. Biol. Chem.* **260,** 8942 (1985).
42. Moura, J. J. G., Moura, I., Huynh, B. H., Krüger, H.-J., Teixeira, M., DuVarney, R. C., DerVartanian, D. V., Xavier, A. V., Peck, H. D., Jr., and LeGall, J., *Biochem. Biophys. Res. Commun.* **108,** 1388 (1982).
43. Van der Zwaan, J. W., Albracht, S. P. J., Fontijn, R. D., and Slater, E. C., *FEBS Lett.* **179,** 271 (1985).
44. Bossu, F. P., and Margerum, D. W., *Inorg. Chem.* **16,** 1210 (1977).
45. Sakurai, T., Hongo, J.-I., Nakahara, A., and Nakao, Y., *Inorg. Chim. Acta* **46,** 205 (1980).
46. Moore, G. D., Pettigrew, G. W., and Rogers, N. K., *Proc. Natl. Acad. Sci. U.S.A.* **83,** 4998 (1986).
47. Haines, R. I., and McAuley, A., *Coord. Chem. Rev.* **39,** 77 (1981).
48. Busch, D. H., *Acct. Chem. Res.* **11,** 392 (1978).
49. Fernandez, V. M., Hatchikian, E. C., and Cammack, R., *Biochim. Biophys. Acta* **832,** 69 (1985).
50. Dietrich-Buchecker, C. O., Kern, J.-M., and Sauvage, J. P., *J. Chem. Soc. Chem. Commun.* 760 (1985).
51. Lindahl, P. A., Kojima, N., Hausinger, R. P., Fox, J. A., Teo, B. K., Walsh, C. T., and Orme-Johnson, W. H., *J. Am. Chem. Soc.* **106,** 3062 (1984).
52. Scott, R. A., Wallin, S. A., Czechowski, M., DerVartanian, D. V., LeGall, J., Peck, H. D., Jr., and Moura, I., *J. Am. Chem. Soc.* **106,** 6864 (1984).
53. DerVartanian, D. V., Kruger, H. J., Peck, H. D., Jr., and LeGall, J., *Rev. Port. Quim.* **27,** 70 (1985).
54. Albracht, S. P. J., Kröger, A., Van der Zwaan, J. W., Unden, G., Böcher, R., Mell, H., and Fontijn, R. D., *Biochim. Biophys. Acta* **116** (1986).
55. Sugiura, Y., Kuwahara, J., and Suzuki, T., *Biochem. Biophys. Res. Commun.* **115,** 878 (1983).
56. Tan, S. L., Fox, J. A., Kojima, N., Walsh, C. T., and Orme-Johnson, W. H., *J. Am. Chem. Soc.* **106,** 3064 (1984).
57. Johnson, M. K., Zambrano, I. C., Czechowski, M. H., Peck, H. D. Jr., DerVartanian, D. V., and LeGall, J., *Biochem. Biophys. Res. Commun.* **128,** 220 (1985).
58. Kim, D.-H., and Holten, D., *Chem. Phys.* **75,** 305 (1983).

59. Shelnutt, J. A., Alston, K., Ho, J. Y., Yu, N. T., and Yamamoto, T., *Biochemistry* **25,** 620 (1986).
60. Findsen, E. W., Alston, K., Shelnutt, J. A., and Ondria, M. R., *J. Am. Chem. Soc.* **108,** 4009 (1986).
61. Tolman, C. A., *J. Am. Chem. Soc.* **94,** 2994 (1972).
62. Dilworth, J. R., *In* "Sulfur and its Relevance to Geo-, Bio- and Cosmosphere and Technology: Studies in Inorganic Chemistry" (A. Müller, ed.), Vol. 5. Elsevier, New York, 1984.
63. Schneider, K., Cammack, R., Schlegel, H. G., and Hall, D. O., *Biochim. Biophys. Acta* **578,** 445 (1979).
64. Van der Zwaan, J. W., Albracht, S. P. J., Fontijn, R. D., and Roelofs, Y. B. M., *Biochim. Biophys. Acta* **872,** 208 (1986).
65. Cammack, R., Patil, D. S., Hatchikian, E. C., and Fernandez, V. M., *Biochim. Biophys. Acta* **912,** 98 (1987).
66. Adams, M. W. W., Mortenson, L. E., and Chen, J.-S., *Biochim. Biophys. Acta* **594,** 105 (1981).
67. Van der Westen, H. M., Mayhew, S. G., and Veeger, C., *FEMS Microbiol. Lett.* **7,** 35 (1980).
68. Cammack, R., Lalla-Maharajh, W. V., and Schneider, K., *In* "Electron Transport and Oxygen Utilization" (C. Ho, ed.), Vol. 2. Elsevier, New York, 1982.
69. Huynh, B. H., Patil, D. S., Moura, I., Teixeira, M., Moura, J. J. G., DerVartanian, D. V., Czechowski, M. H., Prickril, B. C., Peck, H. D., Jr., and LeGall, J., *J. Biol. Chem.* **262,** 795 (1987).
70. Schneider, K., Patil, D. S., and Cammack, R., *Biochim. Biophys. Acta* **748,** 353 (1983).
71. Albracht, S. P. J., Van der Zwaan, J. W., and Fontijn, R. D., *Biochim. Biophys. Acta* **766,** 245 (1984).
72. Cammack, R., Patil, D., and Fernandez, V. M., *Biochem. Soc. Trans.* **13,** 572 (1985).
73. Coffman, R. E., and Buettner, G. R., *J. Phys. Chem.* **83,** 2392 (1979).
74. Berlier, Y. M., Fauque, G., Lespinat, P. A., and LeGall, J., *FEBS Lett.* **140,** 185 (1982).
75. Lissolo, T., Pulvin, S., and Thomas, D., *J. Biol. Chem.* **259,** 11725 (1984).
76. Albracht, S. P. J., Fontijn, R. D., and Van der Zwaan, J. W., *Biochim. Biophys. Acta* **832,** 89 (1985).
77. Hallahan, D. L., Fernandez, V. M., Hatchikian, E. C., and Cammack, R., *Biochim. Biophys. Acta* **874,** 72 (1986).
78. Lespinat, P. A., Berlier, Y., Fauque, G., Czechowski, M., Dimon, B., and LeGall, J., *Biochimie* **68,** 55 (1986).
79. Adams, M. W. W., Jin, S. L. C., Chen, J. S., and Mortenson, L. E., *Biochim. Biophys. Acta* **869,** 37 (1986).
80. Moura, J. J. G., Teixeira, M., Moura, I., and LeGall, J., *In* "Bioinorganic Chemistry of Nickel" (J. R. Lancaster, Jr., ed.). VCH Publ. Deerfield Beach, Florida, 1988 (in press).
81. Hoberman, H. D., and Rittenberg, D., *J. Biol. Chem.* **147,** 211 (1943).
82. Schneider, K., Schlegel, H. G., and Jochim, K., *Eur. J. Biochem.* **138,** 533 (1984).
83. Gunsalus, R. P., and Wolfe, R. S., *FEMS Microbiol. Lett.* **3,** 191 (1978).
84. Ellefson, W. L., Whitman, W. B., and Wolfe, R. S., *Proc. Natl. Acad. Sci. U.S.A.* **79,** 3707 (1982).
85. Hausinger, R. P., Orme-Johnson, W. H., and Walsh, K. M., *Biochemistry* **23,** 801 (1984).
86. Diekert, G., Klee, B., and Thauer, R. K., *Arch. Microbiol.* **124,** 103 (1980).
87. Whitman, W. B., and Wolfe, R. S., *Biochem. Biophys. Res. Commun.* **92,** 1196 (1980).

88. Pfalz, A., Jaun, B., Fässler, A., Eschenmoser, A., Jaenchen, R., Gilles, H. H., Diekert, G., and Thauer, R. K., *Helv. Chim. Acta* **65,** 828 (1982).
89a. Scott, R. A., Hartzell, P. L., Wolfe, R. S., LeGall, J., and Cramer, S. P., *In* "Frontiers in Bioinorganic Chemistry" (A. V. Xavier, ed.), p. 20. VCH Publ., Weinheim, FRG, 1985.
89b. Diakun, G. P., Piggott, B., Tinto, H. J., Fuchs, D. A., and Thauer, R. K., *Biochem. J.* **232,** 281 (1985).
89c. Eidsness, M. K., Sullivan, R. J., Schwartz, J. R., Hartzell, P. L., Wolfe, R. S., Flank, A. M., Cramer, S. P., and Scott, R. A., *J. Am. Chem. Soc.* **108,** 3120 (1986).
90. Albracht, S. P. J., Ankel-fuchs, D., Van der Zwaan, J. W., Fontijn, R. D., and Thauer, R. K., *Biochim. Biophys. Acta* **870,** 50 (1986).
91. Keltjens, J. T., Whitman, W. B., Caerteling, C. G., van Kooten, A. M., Wolfe, R. S., and Vogels, G. D., *Biochem. Biophys. Res. Commun.* **108,** 495 (1982).
92. Diekert, G., and Thauer, R. K., *J. Bacteriol.* **136,** 597 (1978).
93. Diekert, G., Graf, E. G., and Thauer, R. K., *Arch. Microbiol.* **122,** 117 (1979).
94. Ragsdale, S. W., and Wood, H. G., *J. Biol. Chem.* **260,** 3970 (1985).
95. Ragsdale, S. W., Ljungdahl, L. G., and DerVartanian, D. V., *Biochem. Biophys. Res. Commun.* **108,** 658 (1982).
96. Ragsdale, S. W., Ljungdahl, L. G., and DerVartanian, D. V., *Biochem. Biophys. Res. Commun.* **115,** 658 (1983).
97. Ragsdale, S. W., Wood, H. G., and Antholine, W. E., *Proc. Natl. Acad. Sci. U.S.A.* **82,** 6811 (1985).
98. Ragsdale, S. G., Wood, H. G., Morton, T. A., Ljungdahl, L. G., and DerVartanian, D. V., *In* "Bioinorganic Chemistry of Nickel" (J. R. Lancaster, Jr., ed.). VCH Publ., Deerfield Beach, Florida, 1988 (in press).
99. Mege, R.-M., and Bourdillon, C., *J. Biol. Chem.* **260,** 14701 (1985).
100. Cammack, R., Rao, K. K., Serra, J., and Llama, M. J., *Biochimie* **68,** 93 (1986).
101. Cammack, R., Kovacs, K., McCracken, J., and Peisach, J., unpublished observations.
102. Fischer, F., Lieske, R., and Winzer, K., *Biochem. Z.* **245,** 2 (1932).
103. Ragsdale, S. W., Wood, H. G., Morton, T. A., Ljungdahl, L. G., and DerVartanian, D. V., *In* "Bioinorganic Chemistry of Nickel" (J. R. Lancaster, Jr., ed.). VCH Publ., Deerfield Beach, Florida, 1988 (in press).
104. Crabtree, R. H., *Inorg. Chim. Acta* **125,** L7–L8 (1986).